Theoretical and Comparative Study of the Complex [RuCl₃(H₂O)₂(Gly)] by Density Functional Theory

Kátia Meirelles D. de Sousa[1]*, Marcio Adriano S. Chagas[2], Jesyca Mayra F. D. dos Santos[1], Anderson D. Galvão[1], Fabrício Tarso de Moraes[1], Andressa Teixeira Barros Nunes Ribeiro[1], Dário Batista Fortaleza[1], Kelly Aparecida da Encarnação Amorim[1], Wagner B. dos Santos[1]

[1]Materials Research Lab, Federal University of Mato Grosso—Campus II, Barra do Garças, Brazil
[2]Institute of Chemistry, Brasília University, UNB, Brasília, Brazil
Email: *katiamds0@gmail.com, wbsantos@ufmt.br

Abstract

In this work, the use of computational methods was essential to distinguish the three possible isomeric structures of the $[RuCl_3(H_2O)_2(Gly)]$ molecule. The characterization of these molecules was performed using IR, NMR and UV-VIS simulations. Some calculations related to the optimization of structures and properties such as chemical hardness and dipole moment were also conducted. The fac-cis isomer presented promising data when compared to the experimental data, indicating that this is the likely experimentally synthesized isomer. This study demonstrates the technical utility of the computational calculations by virtue of situations that prevent the realization of X-ray diffraction.

Keywords

Computational Methods, Isomeric Structures, Simulations

1. Introduction

Computational calculations are widely used in research to confirm geometric structures and to determine the properties of coordination compounds [1] [2] [3] [4], especially in cases where obtaining a single crystal for X-ray diffraction is not possible [5] [6] or inconclusive [3] [7].

Chagas [8] began to develop the study of the complex $[RuCl_3(H_2O)_2(Gly)]$ in 2012. In biological tests performed by Salama [9], Chagas [8] observed the po-

tential Leishmanicidal activity of its complex. Martínez *et al.* [10], Iniguez *et al.* [11] and Barbosa *et al.* [12] demonstrated that some of their ruthenium compounds exhibited improved antileishmanial activity compared with the reference compound and their free ligand.

Structural variations depending on the size of the molecule, the position of the ligands and their spatial characteristics such as flatness and three-dimensionality help to understand the action of these molecules in the biological environment, as the interaction of a molecule with a biological receptor depends on this type of structural information [13] [14]. Previous research has shown the utility and exploitation of structural knowledge in areas such as catalytic activity and the use of computational calculations in these studies [15] [16]. Gianferrara, Bratsos and Alessio [17] give a good account of the conditions mentioned in the paragraph beginning, based on some examples such as cisplatin and ruthenium compounds (NAMI-A and KP1019), which are anticancer drugs currently in use and under development, respectively.

This study used computational methods to determine the possible geometric isomers of the compound $[RuCl_3(H_2O)_2(Gly)]$, in comparison with experimental data, illustrating the usefulness of computational methods to elucidate the possible geometrical structures of a compound in situations in which a single crystal for X-ray diffraction cannot be obtained.

2. Methodology

All calculations were performed using the Gaussian program package 09 [18]. The geometries were optimized by the DFT method (Density Functional Theory) and the functional hybrid meta-GGA M06-2x [19], and confirmed by vibrational analysis. The basis set used was 6-311++G(d,p) [20] for all atoms except for Ruthenium, which was treated with the basis sets SDD (Stuttgart/double-ζ Dresden) and ECP (effective core potential) for the innermost electrons of the ruthenium atom [21]. The harmonic vibrational frequencies were calculated with the analytical second derivative, without the presence of imaginary frequencies. For the calculations of 35 excited states, the time dependent method (TDDFT) with an open layer was used with a polarized solid model to determine the effect of the solvent water molecule through IEF (integral equation formalism). For the comparison of nuclear magnetic resonance, the calculation was performed by the GIAO method (Atomic Orbital Measure Independent) [22] for ^{13}C and ^{1}H in the presence of the solvent water. All DFT calculations employed the keyword int (grid = ultrafine). All calculations were performed at the Federal University of Mato Grosso, *Laboratório de Estudos de Materiais*. All experimental data were obtained for comparison of the findings [8].

3. Results and Discussion

The $[RuCl_3(H_2O)_2(Gly)]$ molecule described by Chagas [8], can generate three

possible geometric isomers: *fac-cis*-diaquotrischloroglycinatoruthenium III, *mer-cis*-diaquotrischloroglycinatoruthenium III and *mer-trans*-diaquotrischloroglycinatoruthenium III. As shown in Figure 1.

To determine which isomer was synthesized by Chagas [8], computational methods were used to investigate the characteristics of each isomer compared to the experimental data.

3.1. Energy of the Geometrical Isomers

Table 1 shows the data obtained from the energy optimization of each isomer. The data show that the *mer-trans* isomer showed the largest relative difference when compared to the *fac-cis* molecule with the lowest energy. The *fac-cis* molecule, with lower energy compared to the other two isomers, had greater stability. However, the energies of the three structures were very close and the lowest energy does not guarantee formation of the compound experimentally. Thus, IR, UV-vis and NMR simulations were performed to elucidate the structure [5] [6] [23].

3.2. Infrared Simulation

The infrared frequencies of the three isomers showed similar values to each other. It was also observed that, when compared to the experimental data, the *fac-cis* and *mer-trans* isomers demonstrated a closer approximation as show in Table 2.

The *fac* isomer showed lower frequencies than the *mer* isomers for the same bandwidth allocations in regions below 1000 cm^{-1}. However, a difference was

**Molecules**

1. *fac-cis*-diaquotrischloroglycinatoruthenium III

2. *mer-cis*-diaquotrischloroglycinatoruthenium III

3. *mer-trans*-diaquotrischloroglycinatoruthenium III
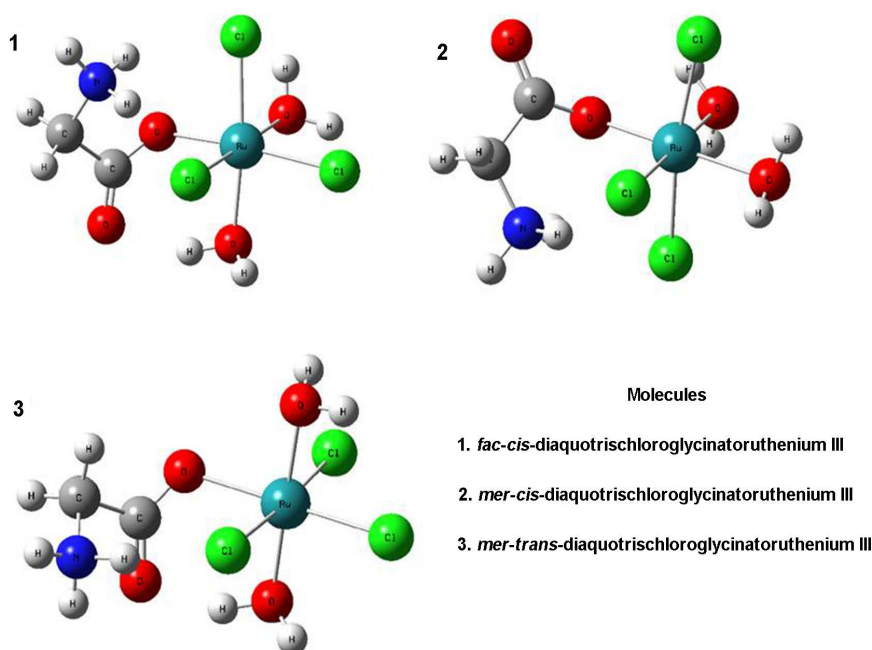
Figure 1. Structure of the molecule isomers [RuCl$_3$(H$_2$O)$_2$gly].

Table 1. Relative energies of isomers of the molecule [RuCl$_3$(H$_2$O)$_2$gly].

Molecules	Optmization energy (Hartree)	Relative energies (kCal·mol^{-1})
fac-cis	−1912.7912080	0
mer-cis	−1912.7794975	7,35
mer-trans	−1912.7661652	15,71

Table 2. Calculated frequency by DFT of isomers [RuCl$_3$(H$_2$O)$_2$(Gly)], and FTIR$_{med}$ (4000 - 600 cm^{-1}) with approximate assignment bands.

(*fac-cis*)	(*mer-cis*)	(*mer-trans*)	Experimental	Assigned bands
1791	1848	1730	1664	va (COO$^-$)
1395	1290	1454	1388	vs (COO$^-$)
1665 - 1595	1667 - 1613	1654 - 1589	1571	δ(NH$_3^+$)
1510	1516	1513	1490	δs(NH$_3^+$)
1479	1472	1491	1441	δ(CH$_2$)
1344	1373	1348	1334 - 1322	ρw(CH$_2$)
1118	1112	1125	1155 - 1110	ρr(NH$_3^+$)
1015	1027	1003	1043	ν (C-N) + ν (C-C)
905	910	924	927	ρr(CH$_2$)
871	894	897	889	ν (CCN)
676	-----	-----	684	ρw(COO$^-$)
617	635	647	607	δ(COO$^-$)

Not observed. va: Asymmetrical stretch; vs: Symmetrical stretch; δa: Asymmetrical bending; δs: symmetrical bending; ρw: Wagging deformation; ρr: Rocking deformation.

not observed between *mer-trans* and *mer-cis*, which did not conform to any general pattern.

$$RMS = \sqrt{\frac{1}{n-1}\sum_{i}^{n}\left(v_i^{cal} - v_i^{exp}\right)^2}$$

The root mean square error (RMSE) between the experimental and the calculated frequency of the molecules were 42.44 cm^{-1} (*fac-cis*), 75.67 cm^{-1} (*mer-cis*) and 37.36 cm^{-1} (*mer-trans*), with the lowest RMSE found for the *mer-trans* molecule, according to the above equation [24]. The overestimated values of the calculated frequency were due to neglecting anharmonicity. The calculation was performed on a single molecule, disregarding intermolecular interactions [25].

The theoretical and experimental spectra in **Figure 2** and **Figure 3** showed characteristic peaks related to the glycine molecule and the compound. The carboxylate group showed variations between asymmetric and symmetric peaks, which assisted in the distinction of the three isomeric structures of the theoretical spectra as *fac-cis* (396 cm^{-1}), *mer-cis* (558 cm^{-1}) and *mer-trans* (276 cm^{-1}). This distinction was observed in a previous work was well Alam *et al.* [26]. The
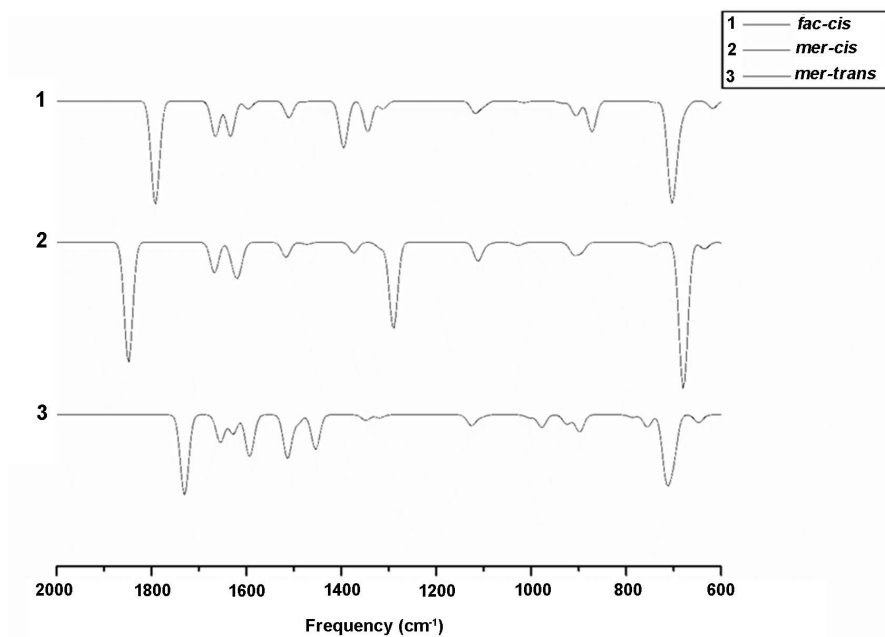
Figure 2. Theoretical spectrum.
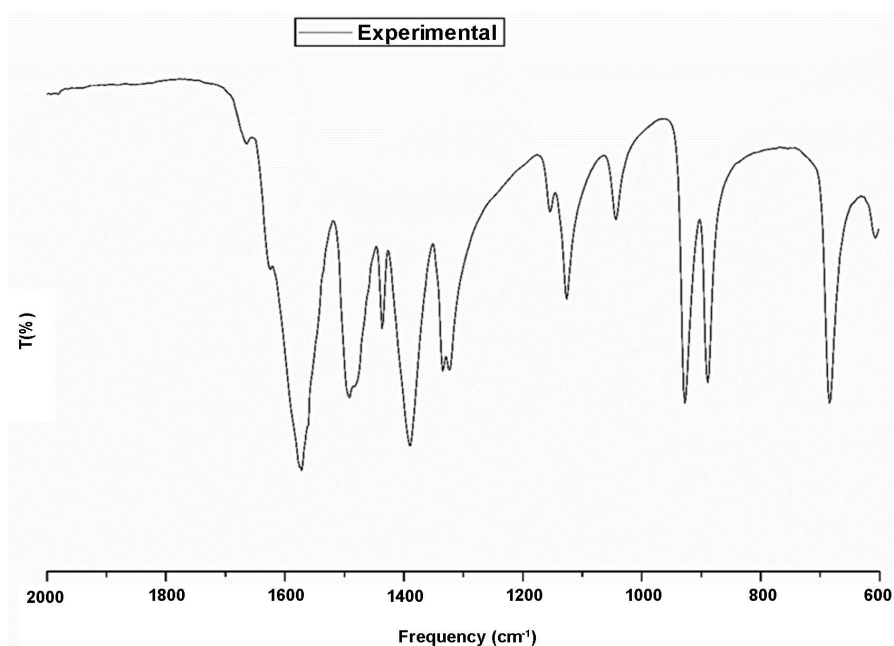
Figure 3. Experimental spectrum.

experimental spectrum showed a variation between asymmetric and symmetric peaks of 276 cm^{-1}. The peak at 676 cm^{-1} was assigned to a "wagging" group (COO^{-}) in the *fac-cis* isomer and was not observed in the *mer* isomers.

3.3. Ultraviolet-Visible Simulation

Table 3 shows the data on electron density-related oscillator strength. Ligand charge transfer to the metal (LMCT) can be evidenced by the HOMO and

Table 3. Electronic density of the molecular frontier orbitals.

Isomers	Homo (orbitals)	Characteristics	Lumo (orbitals)
fac-cis		State 16 Orbital $58\beta \rightarrow 64\beta$ Energy 7.59 (eV)	
mer-cis		State 14 Orbital $59\beta \rightarrow 64\beta$ Energy 7.08 (eV)	
mer-trans		State 14 Orbital $60\beta \rightarrow 64\beta$ Energy 6.96 (eV)	
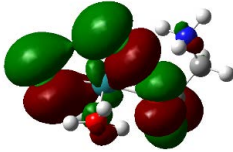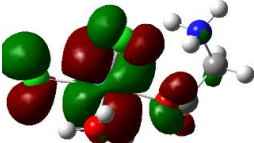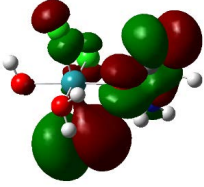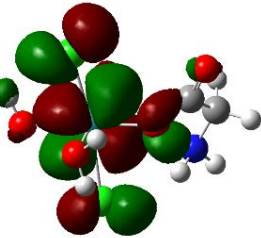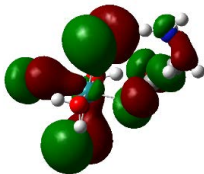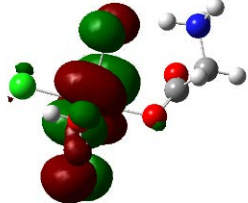
LUMO, referring to the excited states shown in Table 4. The excited state closest to the experimental value was presented by the *fac-cis* molecule.

The values related to states 19 and 26 (*fac-cis*), 19 and 22 (*mer-cis*) and 22 and 27 (*mer-trans*) show π-π* type transitions relating to the glycine binder. The greatest contribution of the chlorides to the metal center occurred in states 19, 16 and 19 of the *fac-cis* structures, *mer-cis* and *mer-trans*, respectively.

3.4. Molecular Properties

The HOMO is the occupied orbital with the highest energy that has the ability to donate electrons, while the LUMO is the unoccupied orbital with the least energy that has the ability to accept electrons; the difference between them can explain charge transfer within a molecule [27] [28]. The HOMO and LUMO data energies as well as their differences are shown in Table 5.

The range of energy between HOMO and LUMO as well as the hardness and chemical dipole moment may provide additional information. The *fac-cis* molecule had the largest energy difference and greater chemical hardness, making it more stable kinetically and less favorable to adding electrons to LUMO or extracting electrons from HOMO, *i.e.* this molecule had low chemical reactivity [29] [30].

The dipole moment implies that the higher the stronger value is an intermolecular interaction [30], The *mer-trans* molecule should form stronger intermolecular bonds than the other two isomers, for example with other molecules or DNA bases, as shown previously Pramanik *et al.* [30] and Das *et al.* [31].

Table 4. Excitation energies (eV), Oscillator strength (f) and wave length (nm) calculated and experimental.

Molecules	States	λ (nm)	eV	f	exp
fac-cis	13	314.98	3.9363	0.0162	
	16	287.49	4.3127	0.0260	290 (LMCT)
	19	257.63	4.8124	0.0087	
	26	238.53	5.1979	0.0093	
mer-cis	14	319.96	3.8750	0.0101	
	16	304.82	4.0675	0.0161	
	19	263.97	4.6969	0.0292	
	22	251.81	4.9236	0.0079	230 (π-π*)
mer-trans	14	321.58	3.8555	0.0119	
	19	283.60	4.3718	0.0170	
	22	257.28	4.8190	0.0223	
	27	244.79	5.0648	0.0337	

Table 5. Calculated data of some molecular properties.

Molecules	Homo eV	Lumo eV	Homo-lumo gap Δ(eV)	Chemical hardness (η)	Dipole moment μ (Debye)
fac-cis	−8.2584	−2.2746	5.9838	2.9919	7.6920
mer-cis	−8.2682	−2.5070	5.7612	2.8806	6.3862
mer-trans	−7.7153	−2.2888	5.4265	2.7133	12.5112

According to the Koopman theorem, the chemical hardness η can be described by the following equation, $\eta = \dfrac{E_{Lumo} - E_{Homo}}{2}$ [32].

3.5. Nuclear Magnetic Resonance Simulation (nmr)

Table 6 is presented the magnetic resonance of ^{13}C and ^{1}H in comparison with experimental data.

The NMR theoretical data indicate overestimated values. These overestimated values can be explained by the method and the basis set, resulting in poor results [33]. Another explanation for such high values is that the simulation was performed on a single molecule, meaning that various types of chemical interactions were not considered theoretically [25].

The NMR data for the *mer-cis* isomer provided a close approximation to the experimental data of the group (COO⁻), but the other NMR results were poorly related to the other two structures. Therefore, a correction of the basis sets and/or the method may provide better results in general.

4. Conclusions

Although some experimental data showed overestimated values, the spectral characteristics were maintained according to the experimental data.

Table 6. Magnetic resonance ^{13}C and ^{1}H.

Parameters	fac-cis	mer-cis	mer-trans	Experimental
$C^-_{(COO)}$	192.15	188.93	193.77	172.61
$C_{(CH_2)}$	43.93	47.06	44.69	41.69
$H_{(CH_2)}$	1.85	3.87	2.82	3.45
	2.39	5.84	3.35	-
$H_{(NH_3)}$	5.07	5.50	3.60	4.64
	6.52	6.72	4.05	4.71

The *fac-cis*-diaquotrischloroglycinatoruthenium III and *mer-trans-diaquotrischloroglycinatoruthenium* III isomer presented data indicating greater stability compared to the other two isomers and was confirmed by optimizing data from the UV-vis simulation, the energy of the frontier orbitals and the chemical hardness, which supported its greater stability.

The *fac-cis*-diaquotrischloroglycinatoruthenium III and *mer-trans-diaquotrischloroglycinatoruthenium* III isomer presented the lowest RMSE in comparison with the other structures. The difference between the RMSE of the *mer-trans* and *fac-cis* isomers was relatively small compared to the *mer-cis* isomer, which had the highest value. Thus, observing only the frequency values cannot differentiate between two isomers, but allowed us to discard the *mer-cis* isomer, which showed the worst results.

The observation of the theoretical spectrum suggests the *mer-trans* structure. The *mer-trans* structure showed higher reactivity compared to the other structures, which implies that this molecule can be modified easily as a function of applied energy compared to the other two structures.

Analyzing the results in general, the *fac-cis*-diaquotrischloroglycinatoruthenium III isomer presented results suggesting that this was the molecule synthesized by Chagas [8].

The data relating to the properties of these three molecules may assist in future studies addressing structural modifications and interactions with the biological environment, since the molecule $[RuCl_3(H_2O)_2(Gly)]$ has been shown to possess antileishmanial activity.

Acknowledgements

Supporting Information

The orientation of the three structures is presented.

References

[1] Chong, E., Xue, W., Storr, T., Kennepohl, P. and Schafer, L.L. (2015) Pyridonate-Supported Titanium(III). Benzylamine as an Easy-To-Use Reductant. *Organometallics*, **34**, 4941-4945. https://doi.org/10.1021/acs.organomet.5b00469

[2] El-Sonbati, A.Z., Diab, M.A., Shoair, A.F., El-Bindary, A.A. and Barakat, A.M.

(2016) Potentiometric, Thermodynamics and Theoretical Calculations of Some Rhodanine Derivatives. *Journal of Molecular Liquids*, **216**, 821-829.
https://doi.org/10.1016/j.molliq.2016.01.084

[3] Sheng, H.W., Luo, W.K., Alamgir, F.M., Bai, J.M. and Ma, E. (2006) Atomic Packing and Short-To-Medium-Range Order in Metallic Glasses. *Nature*, **439**, 419-425.

[4] Bertoli, A.C., Garcia, J.S., Trevisan, M.G., Ramalho, T.C. and Freitas, M.P. (2016) Interactions Fulvate-Metal (Zn2+, Cu2+ and Fe2+): Theoretical Investigation of Thermodynamic, Structural and Spectroscopic Properties. *BioMetals*, **29**, 275-285.
https://doi.org/10.1007/s10534-016-9914-8

[5] Das, P., Sarmah, P.P., Borah, M. and Phukan, A.K. (2009) Low-Spin, Mononuclear, Fe(III) Complexes With P,N Donor Hemilabile Ligands: A Combined Experimental and Theoretical Study. *Inorganica Chimica Acta*, **362**, 5001-5011.
https://doi.org/10.1016/j.ica.2009.08.006

[6] de Oliveira, R.S., Boffo, E.F., Reis, F.C.C., Nikolaou, S., Andriani, K.F., Caramori, G.F. and Doro, F.G. (2016) A Ruthenium Polypyridyl Complex with the Antihypertensive Drug Valsartan: Synthesis, Theoretical Calculations and Interaction Studies with Human Serum Albumin. *Polyhedron*, **114**, 232-241.
https://doi.org/10.1016/j.poly.2015.12.029

[7] Bhattacharjee, J., Das, S., Reddy, T.D.N., Nayek, H.P., Mallik, B.S. and Panda, T.K. (2016) Alkali Metal and Alkaline Earth Metal Complexes with the Bis(borane-diphenylphosphanyl)amido Ligand—Synthesis, Structures, and Catalysis for Ring-Opening Polymerization of ε-Caprolactone. *Zeitschrift für anorganische und allgemeine Chemie*, **642**, 118-127.
https://doi.org/10.1002/zaac.201500593

[8] Chagas, M.A.S., Galvão, A.D., de Moraes, F.T., Ribeiro, A.T.B.N., de Siqueira, A.B., de Assis Salama, I.C.C., Arrais-Silva, W.W., de Sousa, K.M.D., de Sousa Pereira, C.C. and dos Santos, W.B. (2017) Synthesis, Characterization and Analysis of Leishmanicide Ability of the Compound [Ru(Cl)3(H2O)2(gly)]. *Open Journal of Inorganic Chemistry*, **7**, 89-101. https://doi.org/10.4236/ojic.2017.74006

[9] Salama, I.C.C.D.A. (2013) Análise Biológica Dos Compostos Rutênio, Lupeol E Boldina No Modelo Experimental Das Leishmanioses. Dissertação de Mestrado, Universidade Federal do Mato Grosso-Campus Universitário do Araguaia.

[10] Martínez, A., Carreon, T., Iniguez, E., Anzellotti, A., Sánchez, A., Tyan, M., Sattler, A., Herrera, L., Maldonado, R.A. and Sánchez-Delgado, R.A. (2012) Searching for New Chemotherapies for Tropical Diseases: Ruthenium-Clotrimazole Complexes Display High *in Vitro* Activity against Leishmania Major and Trypanosoma Cruzi and Low Toxicity toward Normal Mammalian Cells. *Journal of Medicinal Chemistry*, **55**, 3867-3877. https://doi.org/10.1021/jm300070h

[11] Iniguez, E., Sánchez, A., Vasquez, M.A., Martínez, A., Olivas, J., Sattler, A., Sánchez-Delgado, R.A. and Maldonado, R.A. (2013) Metal-Drug Synergy: New Ruthenium(II) Complexes of Ketoconazole Are Highly Active against Leishmania Major and Trypanosoma Cruzi and Nontoxic to Human or Murine Normal Cells. *Journal of Biological Inorganic Chemistry*, **18**, 779-790.
https://doi.org/10.1007/s00775-013-1024-2

[12] Barbosa, M.I.F., Corrêa, R.S., de Oliveira, K.M., Rodrigues, C., Ellena, J., Nascimento, O.R., Rocha, V.P.C., Nonato, F.R., Macedo, T.S., Barbosa-Filho, J.M., Soares, M.B.P. and Batista, A.A. (2014) Antiparasitic Activities of Novel Ruthenium/Lapachol Complexes. *Journal of Inorganic Biochemistry*, **136**, 33-39.
https://doi.org/10.1016/j.jinorgbio.2014.03.009

[13] Koenig, P.M., Roth, R. and Dietrich, S. (2008) Lock and Key Model System. *EPL*, **84**, 68006/68001-68006/68005. https://doi.org/10.1209/0295-5075/84/68006

[14] Adhireksan, Z., Davey, G.E., Campomanes, P., Groessl, M., Clavel, C.M., Yu, H., Nazarov, A.A., Yeo, C.H.F., Ang, W.H., Dröge, P., Rothlisberger, U., Dyson, P.J. and Davey, C.A. (2014) Ligand Substitutions between Ruthenium-Cymene Compounds Can Control Protein versus DNA Targeting and Anticancer Activity. *Nature Communications*, **5**, Article No. 3462. https://doi.org/10.1038/ncomms4462

[15] Credendino, R., Poater, A., Ragone, F. and Cavallo, L. (2011) A Computational Perspective of Olefins Metathesis Catalyzed by N-Heterocyclic Carbene Ruthenium (Pre)Catalysts. *Catalysis Science & Technology*, **1**, 1287-1297. https://doi.org/10.1039/c1cy00052g

[16] Wu, M., Gill, A.M., Yunpeng, L., Falivene, L., Yongxin, L., Ganguly, R., Cavallo, L. and Garcia, F. (2015) Synthesis, Structural Studies and Ligand Influence on the Stability of Aryl-NHC Stabilised Trimethylaluminium Complexes. *Dalton Transactions*, **44**, 15166-15174. https://doi.org/10.1039/C5DT00079C

[17] Gianferrara, T., Bratsos, I. and Alessio, E. (2009) A Categorization of Metal Anticancer Compounds Based on Their Mode of Action. *Dalton Transactions*, No. 37, 7588-7598. https://doi.org/10.1039/b905798f

[18] Frisch, M.J., Trucks, G.W., Schlegel, H.B., Scuseria, G.E., Robb, M.A., Cheeseman, J.R., Scalmani, G., Barone, V., Mennucci, B., Petersson, G.A., Nakatsuji, H., Caricato, M., Li, X., Hratchian, H.P., Izmaylov, A.F., Bloino, J., Zheng, G., Sonnenberg, J.L., Hada, M., Ehara, M., Toyota, K., Fukuda, R., Hasegawa, J., Ishida, M., Nakajima, T., Honda, Y., Kitao, O., Nakai, H., Vreven, T., Montgomery Jr., J.A., Peralta, J.E., Ogliaro, F., Bearpark, M.J., Heyd, J., Brothers, E.N., Kudin, K.N., Staroverov, V.N., Kobayashi, R., Normand, J., Raghavachari, K., Rendell, A.P., Burant, J.C., Iyengar, S.S., Tomasi, J., Cossi, M., Rega, N., Millam, N.J., Klene, M., Knox, J.E., Cross, J.B., Bakken, V., Adamo, C., Jaramillo, J., Gomperts, R., Stratmann, R.E., Yazyev, O., Austin, A.J., Cammi, R., Pomelli, C., Ochterski, J.W., Martin, R.L., Morokuma, K., Zakrzewski, V.G., Voth, G.A., Salvador, P., Dannenberg, J.J., Dapprich, S., Daniels, A.D., Farkas, Ö., Foresman, J.B., Ortiz, J.V., Cioslowski, J. and Fox, D.J. (2009) Gaussian 09. Gaussian, Inc. Print., Wallingford.

[19] Zhao, Y. and Truhlar, D.G. (2008) The M06 Suite of Density Functionals for Main Group Thermochemistry, Thermochemical Kinetics, Noncovalent Interactions, Excited States, and Transition Elements: Two New Functionals and Systematic Testing of Four M06-Class Functionals and 12 Other Functionals. *Theoretical Chemistry Accounts*, **120**, 215-241. https://doi.org/10.1007/s00214-007-0310-x

[20] Frisch, M.J., Pople, J.A. and Binkley, J.S. (1984) Self-Consistent Molecular Orbital Methods 25. Supplementary Functions for Gaussian Basis Sets. *The Journal of Chemical Physics*, **80**, 3265-3269. https://doi.org/10.1063/1.447079

[21] Andrae, D., Häußermann, U., Dolg, M., Stoll, H. and Preuß, H. (1990) Energy-Adjustedab Initio Pseudopotentials for the Second and Third Row Transition Elements. *Theoretica Chimica Acta*, **77**, 123-141. https://doi.org/10.1007/BF01114537

[22] Wolinski, K., Hinton, J.F. and Pulay, P. (1990) Efficient Implementation of the Gauge-Independent Atomic Orbital Method for NMR Chemical Shift Calculations. *Journal of the American Chemical Society*, **112**, 8251-8260. https://doi.org/10.1021/ja00179a005

[23] Hashem, E., Platts, J.A., Hartl, F., Lorusso, G., Evangelisti, M., Schulzke, C. and Baker, R.J. (2014) Thiocyanate Complexes of Uranium in Multiple Oxidation States: A Combined Structural, Magnetic, Spectroscopic, Spectroelectrochemical, and

Theoretical Study. *Inorganic Chemistry*, **53**, 8624-8637.

[24] Prabavathi, N., Nilufer, A., Krishnakumar, V. and Akilandeswari, L. (2012) Spectroscopic, Electronic Structure and Natural Bond Analysis of 2-aminopyrimidine and 4-aminopyrazolo[3,4-d]pyrimidine: A Comparative Study. *Spectrochimica Acta Part A*: *Molecular and Biomolecular Spectroscopy*, **96**, 226-241.
https://doi.org/10.1016/j.saa.2012.05.015

[25] Kowalczyk, I. (2014) Synthesis and Characterization of Alkylammonium Zwitterionic Amino Acids Derivatives by FTIR, NMR Spectroscopy and DFT Calculations. *Acta Chimica Slovenica*, **61**, 39-50.

[26] Alam, M.M., Islam, S.M.S., Rahman, S.M.M. and Rahman, M.M. (2010) Simultaneous Preparation of Facial and Meridional Isomer of Cobalt-Amino Acid Complexes and Their Characterization. *Journal of Scientific Research*, **2**, 91-98.

[27] Sert, Y., Ucun, F., El-Hiti, G.A., Smith, K. and Hegazy, A.S. (2016) Spectroscopic Investigations and DFT Calculations on 3-(Diacetylamino)-2-ethyl-3H quinazolin-4-one. *Journal of Spectroscopy*, **2016**, Article ID: 5396439.
https://doi.org/10.1155/2016/5396439

[28] Chaitanya, K. (2012) Molecular Structure, Vibrational Spectroscopic (FT-IR, FT-Raman), UV-Vis Spectra, First Order Hyperpolarizability, NBO Analysis, HOMO and LUMO Analysis, Thermodynamic Properties of Benzophenone 2,4-Dicarboxylic Acid by Ab Initio HF and Density Functional Method. *Spectrochimica Acta Part A*: *Molecular and Biomolecular Spectroscopy*, **86**, 159-173.
https://doi.org/10.1016/j.saa.2011.09.069

[29] Pearson, R.G. (2005) Chemical Hardness and Density Functional Theory. *Journal of Chemical Sciences*, **117**, 369-377. https://doi.org/10.1007/BF02708340

[30] Pramanik, H.A.R., Das, D., Paul, P.C., Mondal, P. and Bhattacharjee, C.R. (2014) Newer Mixed Ligand Schiff Base Complexes from Aquo-N-(2'-Hydroxy Acetophenone) Glycinatocopper(II) as Synthon: DFT, Antimicrobial Activity and Molecular Docking Study. *Journal of Molecular Structure*, **1059**, 309-319.
https://doi.org/10.1016/j.molstruc.2013.12.009

[31] Das, D., Dutta, A. and Mondal, P. (2015) Interaction of Aquated form of Ruthenium(III) Anticancer Complexes with Normal and Mismatch Base Pairs: A Density Functional Theoretical Study. *Computational and Theoretical Chemistry*, **1072**, 28-36. https://doi.org/10.1016/j.comptc.2015.08.020

[32] Shankar, R., Senthilkumar, K. and Kolandaivel, P. (2009) Calculation of Ionization Potential and Chemical Hardness: A Comparative Study of Different Methods. *International Journal of Quantum Chemistry*, **109**, 764-771.
https://doi.org/10.1002/qua.21883

[33] Gontrani, L., Mennucci, B. and Tomasi, J. (2000) Glycine and Alanine: A Theoretical Study of Solvent Effects upon Energetics and Molecular Response Properties. *Journal of Molecular Structure*: *Theochem*, **500**, 113-127.
https://doi.org/10.1016/S0166-1280(00)00390-0